# PRELIMINARY STUDY OF OXIDATION MECHANISMS OF HIGH CR STEELS IN SUPERCRITICAL WATER

**D.M. Artymowicz[1], C. Andrei[3], J. Huang[3], J. Miles[2], W.G. Cook[2], G.A. Botton[3], R.C. Newman[1]**

[1] University of Toronto, Department of Chemical Engineering and Applied Chemistry, 200 College Street, Toronto, Ontario, M5S 3E5, Canada
[2]University of New Brunswick, Department of Chemical Engineering, 15 Dineen Drive, P.O. Box 4400, Fredericton, New Brunswick, E3B 5A3, Canada
[3]McMaster University, Canadian Centre for Electron Microscopy, 1280 Main Street West, Hamilton, Ontario, L4S 4M1, Canada

## Abstract

Two ferritic steels with 14 and 25 wt% Cr were exposed to Supercritical Water (SCW) for 500 hours. Oxidation products were examined by analytical electron microscopy. The 14Cr steel was uniformly covered by a 10 μm-thick, Fe-rich oxide which grew outwards from the original steel/SCW interface. An equally thick dual oxide layer was found underneath the original interface. Two modes of oxidation were observed on the 25Cr steel. The majority of the surface was covered with a submicron, homogeneous Cr-rich protective oxide layer. Additionally, external Fe-rich oxide nodules formed along grain boundaries and polishing lines with mirror-image Cr-rich oxide nodules penetrating into the alloy. Nodule initiation was connected with the pre-exposure steel homogenization treatment, which could have formed undesirable phases along grain boundaries and resulted in local Cr depletion; however the oxidation propagated beyond any possible depleted zone.

## 1. Introduction

Oxidation of steels in SCW shows features of both gaseous and aqueous oxidation, and also has its own unique features that are being explored in this project by high-resolution microscopy and analysis. The eventual goal is to produce new steels with enhanced SCW oxidation resistance.

Ferritic or ferritic-martensitic (F/M) steels have attractive mechanical properties, are thought to be relatively resistant to stress corrosion cracking (SCC) in SCW, and can be alloyed with beneficial elements such as Cr and possibly others (Si, Al, etc.). Optionally, they could be used as coatings rather than monolithic material. As an initial step, two steels with 14 and 25 wt% Cr were fabricated by CANMET and oxidized in neutral, nominally deoxygenated supercritical water at 500$^{o}$C for 500 hours.

When dealing with any oxidation that occurs at relatively low temperature, one should keep in mind the transport mechanisms that could contribute to the compositions and morphologies

observed. The possibility of internal or intergranular oxidation is of particular concern, as it could lead to rapid SCC. For fcc NiCrFe alloys undergoing internal oxidation in steam-hydrogen mixtures at 480°C, complex morphologies develop within a few hours, despite negligible lattice diffusion of Ni or Cr [1]. These morphologies are produced by a combination of inward lattice diffusion of oxygen, internal oxidation of Cr, mechanical extrusion of metal due to compressive stress, and short-circuit diffusion of both oxygen and metal. In the present case of ferrite at 500°C, lattice diffusion of oxygen is again quite rapid, but the tendency of Fe to form a continuous external oxide makes internal oxidation of Cr or other elements less likely, especially with 25% Cr in the alloy. Lattice diffusion of metal is slow, but more rapid than in the NiCrFe example, so it can be expected to give detectable consequences.

## 2. Experimental Procedures

The details of the alloy manufacture, SCW exposure and various microscopic observations are given in another paper at this Workshop [2]. It should be noted that both alloys contained 0.3 wt% Mo and 0.02 wt% C, and were furnace cooled to 850°C from the homogenization temperature before fan cooling; this procedure was acceptable for the 14Cr alloy, but caused precipitation of a grain-boundary phase in the 25Cr alloy; nevertheless, the results on the latter alloy are of general interest. Another relevant issue is surface preparation, which was abrasion to an 800 grit finish – this might be varied in future studies. 500°C is high enough that significant recovery or even recrystallization can occur in the deformed layer from abrasion.

Cross-sectional and surface imaging, as well as sample preparation for transmission electron microscopy (TEM), were carried out on a Zeiss NVision 40 Focused Ion Beam/Scanning Electron Microscope, using the lift-out technique. The TEM observations were performed on a FEI Titan 80-300 instrument fitted with an energy dispersive X-ray spectrometer (Inca model) for elemental mapping and chemical analysis as well as a high-angle annular dark-field detector.

## 3. Results and Discussion

The 14Cr alloy formed a thick oxide with a well-defined segregation of the alloying elements: outward growth of a voided, Fe-rich oxide and inward growth of a denser oxide containing both Fe and Cr, with indications of an internally oxidized zone at the interface of the latter layer with the base metal [2]. In the preliminary work reported here, no TEM of the inner layer or the base metal interface was achieved – the outer oxide will need to be thinned first. But electron transparency was achieved in the outer oxide, which showed a columnar structure with voids and negligible Cr or Mo content – Figures 1-3.

The 25Cr alloy formed a thin, protective oxide over nearly the whole surface, but with spectacular Fe-rich oxide nodules at grain boundaries and at some scratch lines – Figures 4-5. Beneath each Fe-rich nodule is a kind of mirror-image internal nodule of mixed oxide, and there are indications of internal oxidation at the base metal interface (Figure 5b). The nodule formation at grain boundaries occurs near a second phase that has not been conclusively

identified as yet. This must have formed either during the latter stages of the furnace cool from 1200 to 850$^{o}$C, or during insufficiently rapid air cooling below that temperature (the samples for SCW exposure were machined from the centerlines of thicker plates of alloy).

The protective oxide as well as small oxide nodules were successfully imaged by TEM – Figure 6. The nanocrystalline material under the protective oxide is metal, resulting from the effect of the 500$^{o}$C testing temperature on the deformed layer from 800 grit abrasion. In Figure 7 some medium-sized oxide nodules have been captured and analyzed by EDX. The oxide compositions are much as expected. Some of the Cr-rich contrast in these images is not fully understood as yet, but may be due to second phase from heat treatment.

## 4. Conclusions

- The use of FIB and analytical TEM has enormous potential in the study of SCW oxidation.

- The 14Cr steel oxidizes relatively rapidly in SCW, with outer Fe-rich and inner Cr-rich oxide layers.

- The 25Cr steel has very good oxidation resistance in SCW, but grain boundaries can initiate rapid oxidation, apparently due to the presence of a deleterious second phase. This oxidation propagates locally at a rate similar to that of the 14Cr steel. However, it is not certain that Cr depletion due to such a phase is necessary for the propagation of such oxidation.

- There are indications of internal oxidation at the oxidation fronts in both alloys.

## 5. Acknowledgements

This research was funded by NRCan, NSERC and AECL under the Generation IV Energy Technologies program. Discussions with David Guzonas and Wenyue Zheng are gratefully acknowledged. The electron microscopy work was carried out at the Canadian Centre for Electron Microscopy, a facility supported by McMaster University and NSERC.

## 6. References

[1] R.C. Newman and F. Scenini, Another way to think about the critical oxide volume fraction for the internal to external oxidation transition? Corrosion, 64, 721-726 (2008).

[2] W. Cook, J. Miles, J. Li, S. Kuyucak and W. Zheng, “Preliminary analysis of candidate alloys for use in the CANDU-SCWR” (these proceedings).

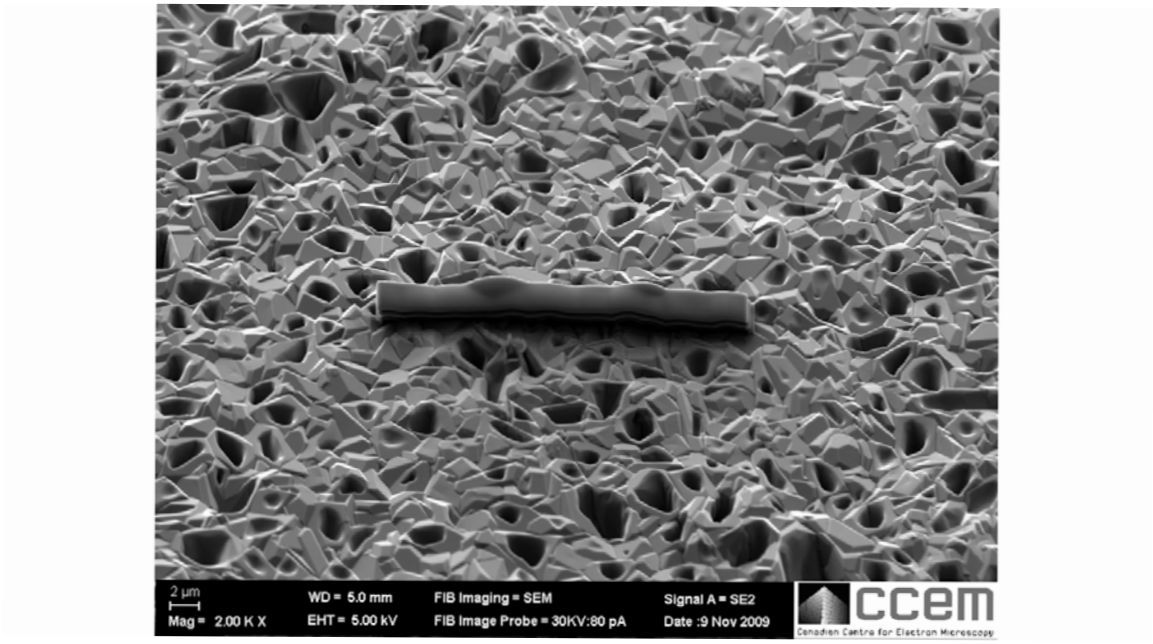


Figure 1 Surface of the oxide on the 14Cr alloy, prepared for FIB sectioning. The elongated strip on the centre of the image is a thin protective coating used for the protection of the topmost surface for the TEM sample preparation. Scale bar: 2 μm.

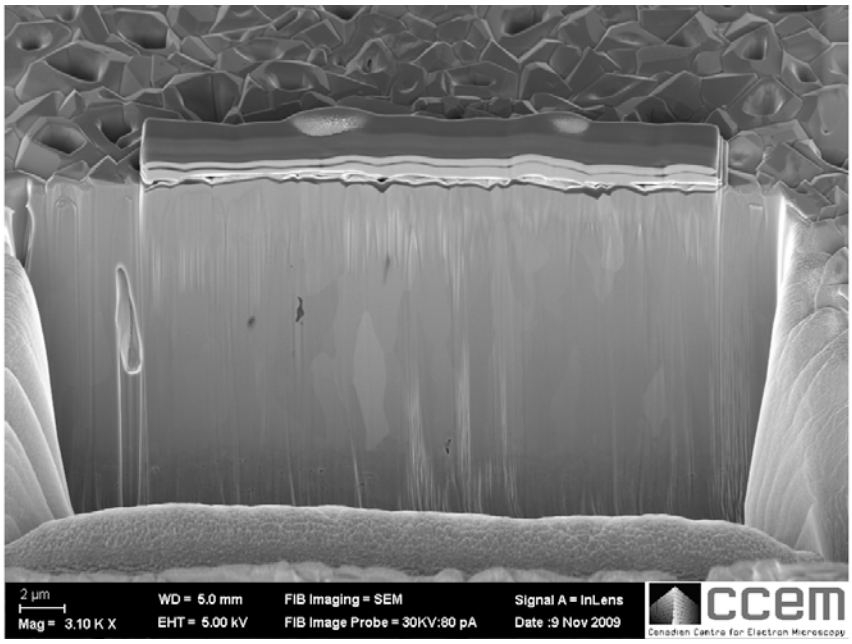


Figure 2 FIB cross-sectional surface of the oxidized 14Cr alloy, showing the outer Fe-rich oxide with indications of its columnar grain structure and presence of voids. Scale bar: 2 μm.

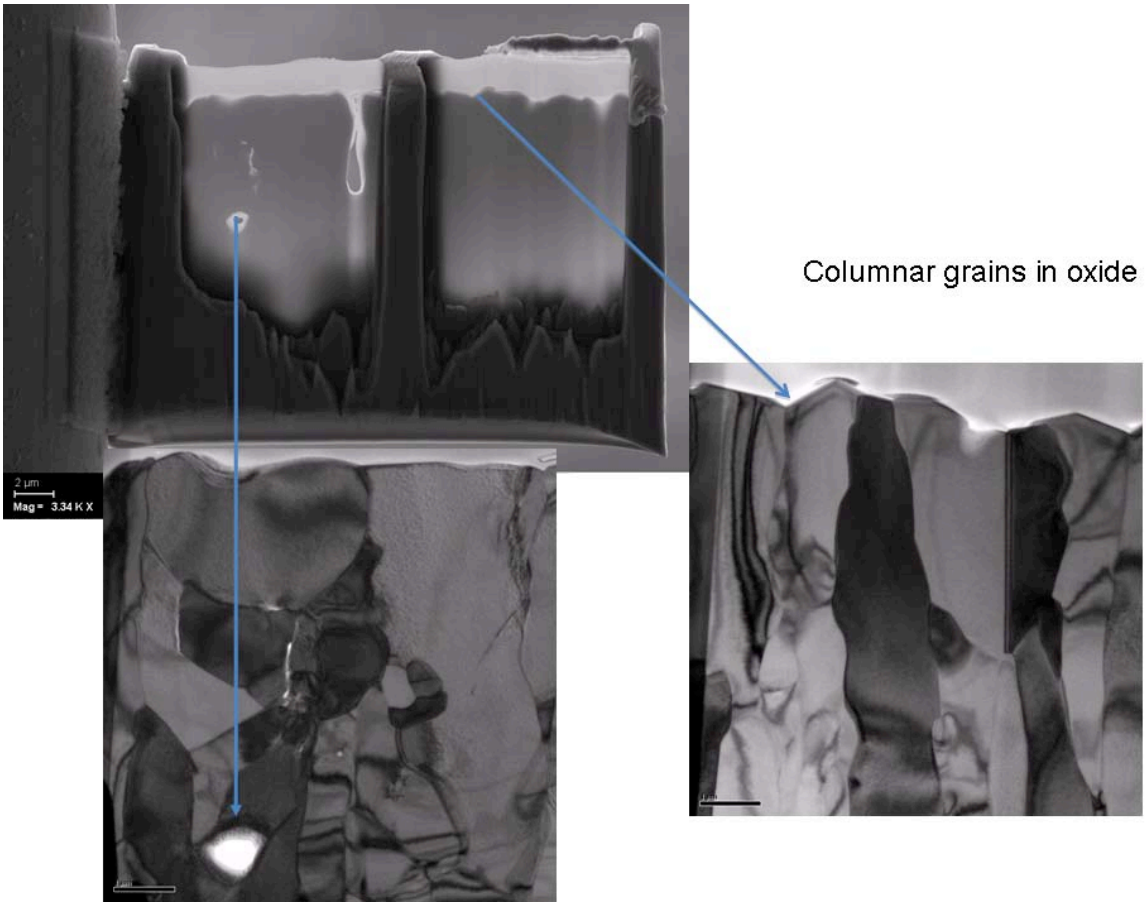


Figure 3 TEM cross-section of the Fe-rich oxide, showing its columnar grain structure and occasional voids. EDX analysis showed only Fe and O. The top bright layer in the cross-section is the protective coating deposited prior to FIB preparation (see Figure 1). Scale bars: top left 2 μm; others 1 μm.

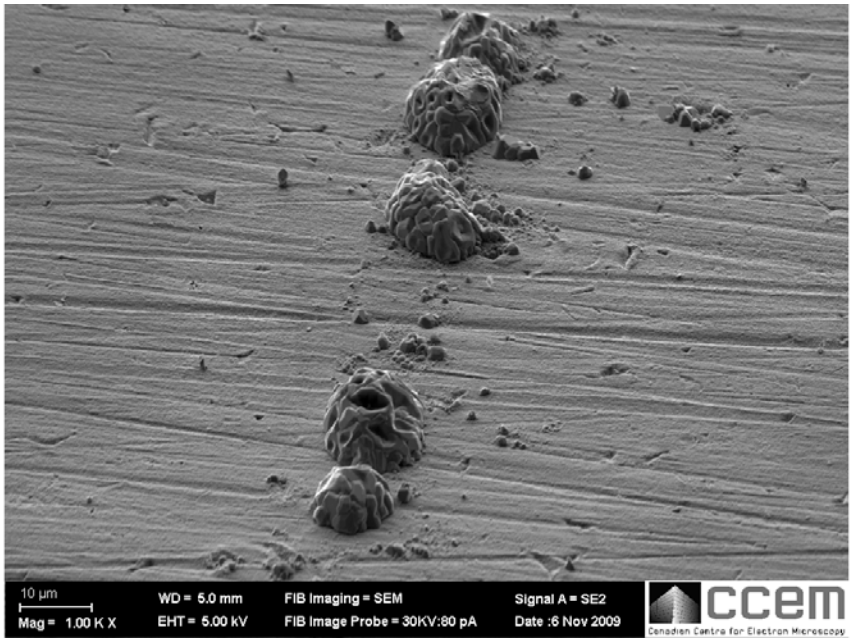


Figure 4 SEM image showing Fe-rich oxide nodules formed at grain boundaries in the oxidized 25Cr alloy. Scale bar: 10 μm.

(a)

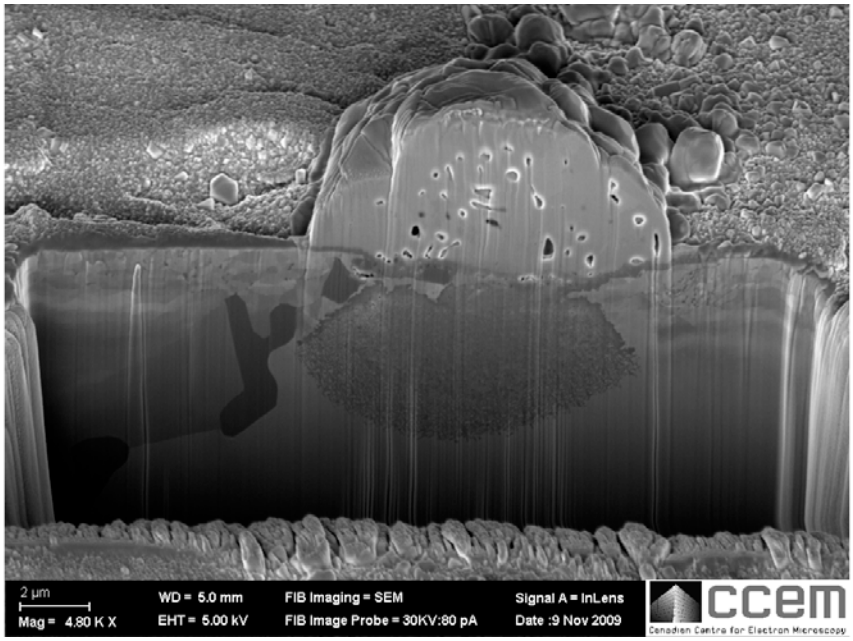


(b)

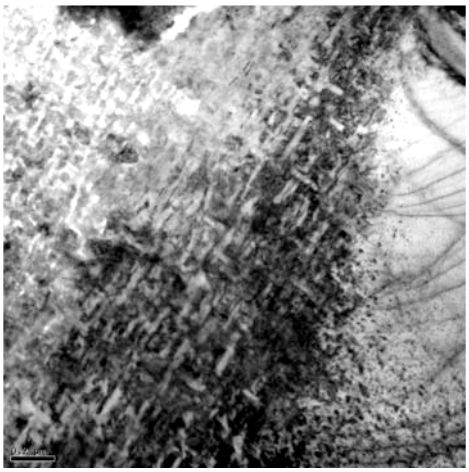

Figure 5 (a) FIB cross-sectional surface of the oxidized 25Cr alloy, showing an outer Fe-rich oxide nodule, inner mirror-image nodule of mixed oxide, and indications of internal oxidation at the base metal interface. To the left can be seen a grain-boundary phase (dark contrast) whose nature is still under investigation. This image also gives an indication of the thickness and morphology of the protective surface oxide. Scale bar: 2 μm. (b) Detail of internally oxidized region by TEM imaging. Scale bar: 0.2 μm.

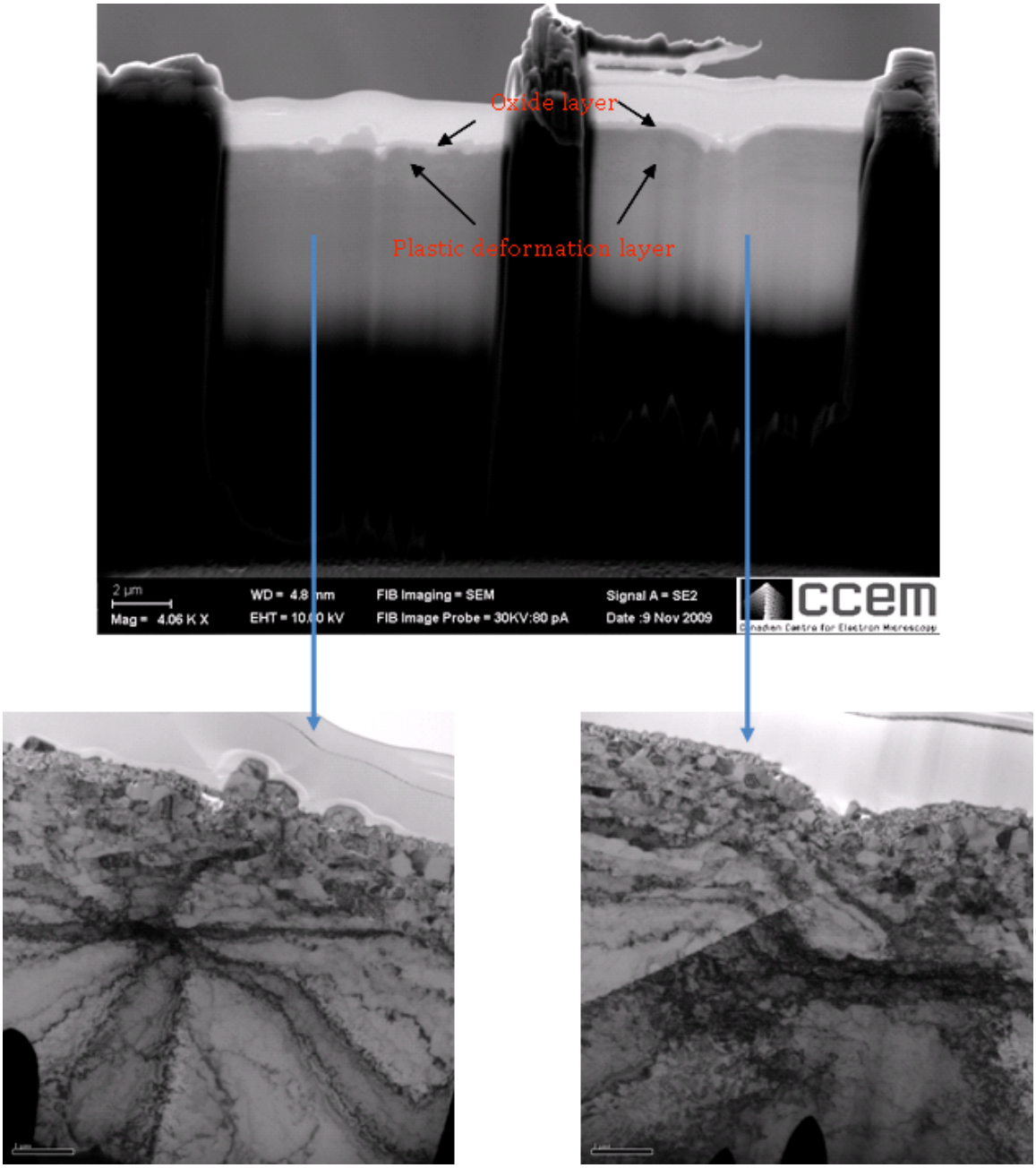


Figure 6 TEM cross-section of a grain boundary in the oxidized 25Cr alloy, showing a small oxide nodule as well as the protective oxide and a nanocrystalline metallic layer that was originally the damaged region from sample abrasion. The topmost bright layer is the protective coating deposited prior to the FIB sample preparation so as to prevent the milling of the thin oxide layer. Scale bars on upper and lower images:
2 µm and 1 µm respectively.

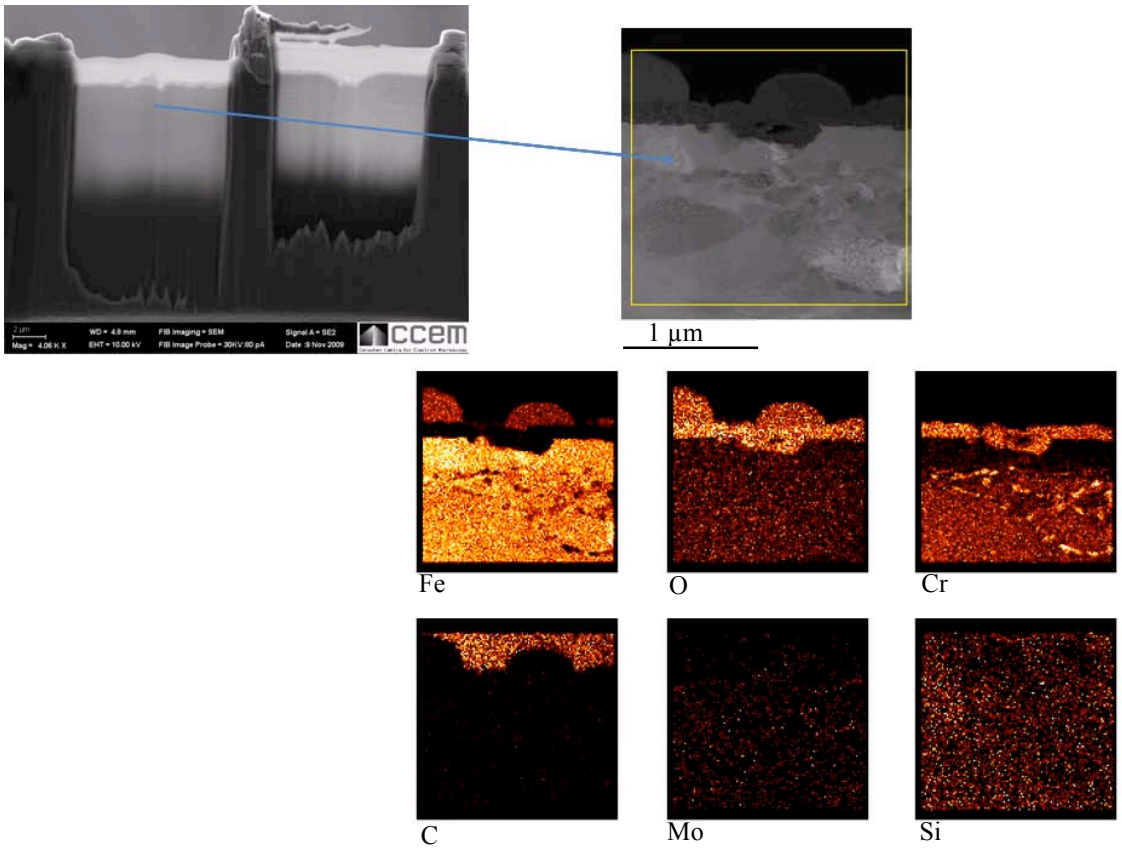


Figure 7 TEM image and EDX elemental mapping analysis of medium-sized nodules near a grain boundary in the oxidized 25Cr alloy. Scale bars: top left 2 μm; top right 1 μm. Magnification on the top right image and all elemental maps is the same.